Libyan Open University Journal of Applied Sciences (LOUJAS)
Volume 2 - Issue 1 - 2026 - Pages 274-289

Thermodynamic Effects of Subcooling and Superheat on a Cascade Cooling System

Adel Mohamed A Kraim
Department of Mechanical Engineering, Faculty of Engineering, Libyan Open University, Tripoli, Libya
*Email:amkraim@yahoo.com

الأثار الثرموديناميكية عند تثبيت درجة حرارة التبريد الدوني و التحميص على منظومة التبريد المتتالي

عادل محمد عبدالحفيظ كريم
قسم الهندسة الميكانيكية، كلية الهندسة، جامعة ليبيا المفتوحة، طرابلس، ليبيا

Received: 18-01-2026; Accepted: 20-03-2026; Published: 10-04-2026

Abstract:
This research presents laboratory results for a cascade refrigeration system CRS to determine the effects of superheating at 4°C on the system's performance rate. The results confirmation curves for the cooling room temperature, suction line pressure, expansion valve opening percentage, and superheat in the low-pressure cycle LPC, and suction line pressure in the high-pressure cycle HPC. The results of valve opening percentage and superheat in LPC when using R32, and the mixture of 90% R32 and 10% R600A by mass, were compared. Also this research proves that the amount of superheat has a significant impact on energy savings and resource sustainability. To avoid energy waste by refrigeration equipment, this research proves the great importance of knowing the optimal value of the superheat in the suction line to maintain the most important element in the refrigeration cycle, which is the compressor, as the entry of the refrigerant liquid into it is avoided for all stages of refrigeration, gradually to reach the required temperature. In the first experiment, the R407c curve decreases from a value of 3.07 bar to 2.83 bar. As for the second experiment in HPC, the suction line pressure shows the highest pressure in the curve for R407c when using the mixture at a value of 3.18 bar. The results confirm that superheat has a direct relationship to reducing the operating cost of CRS and reaching the required temperature in the cooling room in the shortest possible time, by controlling the percentage of opening of the electric valve. Therefore, we recommend focusing on more extensive research regarding the relationship between controlling the valve opening ratio and superheat before the refrigerant enters the compressor.

Keywords: cascade cooling, heat pump, superheat, Subcooling, compressor protection.

الملخص:
يقدم هذا البحث نتائج معملية لنظام تبريد متتالي (CRS) لتحديد تأثير التسخين الفائق عند 4 درجات مئوية على أداء النظام. وقد تم تأكيد النتائج من خلال منحنيات لدرجة حرارة غرفة التبريد، وضغط خط السحب، ونسبة فتح صمام التمدد، والتسخين الفائق في دورة الضغط المنخفض (LPC)، وضغط خط السحب في دورة الضغط العالي (HPC). كما تمت مقارنة نتائج نسبة فتح الصمام والتسخين الفائق في دورة الضغط المنخفض عند استخدام غاز التبريد R32، ومزيج من 90% R32 و10% R600A بالكتلة. ويثبت هذا البحث أيضًا أن كمية التسخين الفائق لها تأثير كبير على توفير الطاقة واستدامة الموارد. ولتجنب هدر الطاقة في معدات التبريد، يؤكد هذا البحث على الأهمية البالغة لمعرفة القيمة المثلى للتسخين الفائق في خط السحب للحفاظ على أهم عنصر في دورة التبريد، وهو الضاغط، حيث يتم تجنب دخول سائل التبريد إليه في جميع مراحل التبريد، وصولًا تدريجيًا إلى درجة الحرارة المطلوبة. في التجربة الأولى، انخفض منحنى R407c من 3.07 بار إلى 2.83 بار. أما في التجربة الثانية في (HPC)، فقد أظهر ضغط خط السحب أعلى قيمة له في منحنى R407c عند استخدام الخليط بقيمة 3.18 بار. تؤكد النتائج أن التسخين الفائق يرتبط ارتباطًا مباشرًا بخفض تكلفة تشغيل نظام التبريد والوصول إلى درجة الحرارة المطلوبة في غرفة التبريد في أقصر وقت ممكن، وذلك من خلال التحكم

في نسبة فتح الصمام الكهربائي. لذا، نوصي بالتركيز على إجراء بحوث أكثر شمولًا حول العلاقة بين التحكم في نسبة فتح الصمام والتسخين الفائق قبل دخول غاز التبريد إلى الضاغط.

الكلمات المفتاحية: التبريد المتتالي، المضخة الحرارية، التسخين الفائق، التبريد الفرعي، حماية الضاغط.

Introduction

In this research, superheat values in the suction line of a cascade refrigeration system CRS were studied, and their effects on room temperature were analyzed. The resulting curves showed the relationships between superheat values and energy consumption, and evaporator pressure. Superheat values in refrigeration systems are an important factor in the efficiency of the cycle and its cooling capacity. This research aims to obtain the most suitable roasting values at the optimal system efficiency through experimental examination of the effects of superheat values in a continuous vapor pressure refrigeration system.

In the first step, using R717 and R744 refrigerants, a thermal economy analysis was applied to the TS-CRS system. Based on the results of the first section, and using an optimized genetic algorithm (GA) implemented in MATLAB, the optimal operating conditions for a specific TS-CRS system were determined [1]. Some important simulation results from simulation and operational tests are presented. The improved control architecture was implemented on a programmable logic controller (PLC) and tested at the plant [2]. The control design focuses on maintaining the refrigerant at 20°C, while ensuring a 5°C superheat at the evaporator outlets, and an intermediate temperature set to the geometric mean of the low-stage evaporator and high-stage condenser temperatures to optimize system efficiency [3]. Furthermore, the extracted optimal solution was compared to a corresponding solution for a basic configuration recently published in the scientific literature which served as the reference design for the same coefficient of performance (COP), operating fluids, cooling capacity, and evaporator temperature (50.00 kW and -17.0 °C, respectively). The comparison showed that the minimum total heat transfer area extracted was approximately 7.3% smaller than the area required in the reference case [4]. It has been shown that improving each of the design parameters of the cascade heat pump is necessary to achieve maximum system performance, which can improve energy efficiency, especially for CRS, by up to 30.88% [5]. The analyses were conducted at the following times: 10:30:00 AM, 11:27:54 AM, 12:25:57 PM, 2:51:00 PM, and 5:17:06 PM. The cooling capacity of the sequential system reached its maximum value (9.29 kW) at noon. Furthermore, the highest efficiency of the solar heating unit was determined to be 49.807% and 49.732%, respectively, at late morning and noon [6]. The cooling capacity values ranged from 4.09 to 5.13 kW. The lowest air temperature inside the cold room was -28°C, while the highest was -5°C. Finally, the results obtained for the R744/R404A combination were found to be consistent with the air temperature conditions inside the cold room, with similar COP values. However, the R744/R404A combination operated at lower cooling capacities, ranging from 2.16 to 3.00 kW [7]. The simulation results show an improvement in the net heat rate of the new cycle of 104.8 kJ/kWh, and an increase in net cycle efficiency of 0.61%. This improvement in the net heat rate of the new cycle is attributed to the improvement of the turbine inlet steam connection to the heat pump, which contributes to an increase in the net heat rate of 14 kJ/kWh [8].

The cascade cooling cycle was analyzed using a computer program developed with the Engineering Equation Solver (EES) software [9]. This study proposes a highly efficient self-contained cascade cooling system for phase separation, operating with a carbon dioxide zetropy mixture. The selection of a high-boiling-point component is analyzed. A novel zetropy mixture consisting of a high percentage of carbon dioxide (R744) with isobutane (R600a) as the carrier fluid is also proposed [10]. The test results indicate that the superheat at the evaporator outlet is the key factor associated with the system's operational stability. When using the plate evaporator, with a superheat of 1.8 °C, instability was observed due to fluid drift through the control window [11]. An optimal superheating temperature for the system's

output power and efficiency is 35 K for a coefficient of expansion of 3.5 and 45 K for a coefficient of expansion of 5 [12]. Simulation studies and experimental trials were conducted to demonstrate the effectiveness of the proposed cascade control strategy, and the results indicate significant improvements in tracking performance and energy efficiency in the constant voltage control system. Compared with other schemes, the proposed cascade control strategy improves energy efficiency by up to 5.8% [13]. The total system lifecycle cost is also reduced by approximately 26.97%. This study provides crucial insights for the development of heat pump/air conditioning systems for a wide range of temperatures and offers a theoretical foundation for promoting green building technologies [14]. The use of the R1270/R170 natural refrigerant pair was found to achieve approximately a 5% better coefficient of performance (COP) and roughly half the CO_2 emissions compared to the use of the R404A/R508B synthetic refrigerant pair [15]. A cascade cooling system model and an air-source cascade heat pump water heater model were built using the Modelica language, and the air-source heat pump water heater model was validated through experimental data [16].

In the ambient temperature range of 243.15 K to 323.15 K, the average improvement in the coefficient of performance (COP) of the new system reaches 34.8%, while the maximum improvement reaches 107.7%, compared to a series heat pump. In the ambient temperature range of 248.15 K to 323.15 K, the new system, when compared to a single-stage heat pump, shows an average improvement in the COP of 25.8%, while the maximum improvement reaches 55.6% [17]. Maintaining an evaporation pressure of 0.7 MPa, the low-toxicity and environmentally friendly refrigerant R245fa was used in this research under different bottom-cycle ratios (Ŧ) and superheating temperatures [18]. The study discusses the optimal operating conditions for different systems and evaluates component costs based on their capacity. The research findings may provide practical guidance for the application of CO_2/C_3H_8 CRS systems equipped with pre-cooling processes [19].

A new semi-sequential heat pump system is proposed, characterized by operational flexibility across varying temperature differences. The system can operate in three modes, single-stage mode, conventional sequential mode, and semi-sequential mode with gradual heating [20]. A two-stage cascade heat pump cycle, operating with two different refrigerants, provides a sustainable solution for raising the condenser temperature above 343 K. In this study, a numerical simulation model was developed to predict the performance of a combined water heating system, based on a solar collector and a two-stage cascade heat pump, under the climatic conditions of Kazakhstan. The numerical simulation of winter climatic conditions was performed using nine refrigerant pairs: R32/R290, R32/R1234yf, R32/R134a, R410A/R290, R410A/R1234yf, R410A/R134a, R744/R290, R744/R1234yf, and R744/R134a [21]. Within the range of chamber temperature variations, cooling capacity and energy efficiency improve by 5.25%–11.36% and 5.29%–9.88%, respectively. 24-hour energy consumption decreases by 2.38%–19.99%. Under varying ambient temperatures, cooling capacity and energy efficiency showed average growth rates of 8.21% and 7.28%, respectively [22]. The cascade system is characterized by a low amount of refrigerant gas used, which is 47 kg of both liquids, which is less than half the amount of refrigerant gas used in the other systems [23].

Material And Methods

For the purpose of testing, CRS was designed and installed for two experiments. In both experiments, R407C was used in the high-pressure cycle, and in the low-pressure cycle, two refrigerants were used. In the first experiment, R32 was used, and in the second experiment, a mixture consisting of (R32 90% & R600A 10% by mass) was used. In this study, computer-controlled electronic expansion valves, an electronic electricity meter, and computer-connected temperature measuring equipment were used to collect experimental data. Based on

superheat values in the experiments, variations of up to 21.3°C were observed in the compressor inlet temperatures at the suction line.

2.1 Theoretical Foundations:

According to the second law of thermodynamics, heat can only flow from a high-temperature environment to a low-temperature environment; the reverse is impossible. Although vapor-compression refrigeration cycles operate on the same principle, they enable heat transfer from a low-temperature room to a high-temperature environment by exploiting changes in the state of the refrigerant. In other words, this occurs through unnatural forced convection. For this reason, another name for vapor-compression refrigeration cycles is "heat pump."

Figure 1 illustrates a sequential refrigeration cycle where the two circuits are connected via a heat exchanger. This exchanger acts as an evaporator in the high-pressure (HPC) cycle and as a condenser in the low-pressure (LPC) cycle. Neglecting kinetic and potential energies, and assuming the heat exchanger is well insulated from the external environment, the heat emitted from the LPC cycle condenser will be equal to the heat received from the HPC cycle evaporator. The refrigerants do not mix in the heat exchanger, the refrigerants in the HPC and LPC systems are not necessarily identical. Therefore, refrigerants with the optimal properties required in each cycle can be used.

In the first stage of this system, compression (5-6) occurs in HPC compressor, condensation (6-7) in the main condenser, expansion (7-8) in HPC expansion valve pressure reducer, and evaporation (8-5) in the heat exchanger evaporator. Similarly, in the second stage of LPC, compression (1-2) occurs in LPC compressor, condensation (2-3) in the heat exchanger condenser, expansion (3-4) in LPC pressure reducer, and evaporation (4-1) in the main evaporator of the cold room.

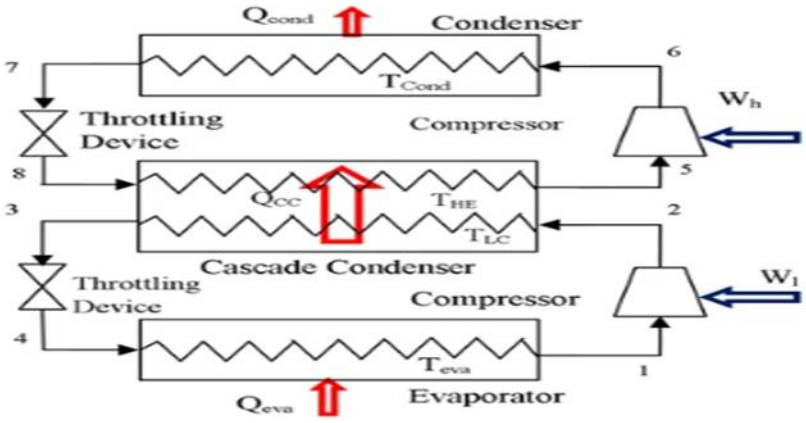

Figure (1) Cascade vapor compression refrigeration cycle scheme

The following auxiliary components were used in the laboratory system employed in this research:

Liquid separator: This separates the liquid and vapor of the refrigerant, preventing the liquid coming from the evaporator from damaging the compressor. It is located between the evaporator and the compressor.

Dryer: This filters water vapor and solid particles that may be present in the refrigerant gas. It is located between the condenser and the expansion element.

Oil separator: This separates the oil from the refrigerant when compressor oil mixes with the refrigerant. Because the amount of oil separated can be significant in high-capacity systems, the oil is returned to the compressor via a bypass line.

Receiver: This is a liquid reservoir used to store excess liquid from the refrigerant gas that liquefies in the condenser. It is located between the condenser and the dryer.

Viewing window: This is used to check for moisture or bubbles in the liquid passing through the expansion element. It is located between the expansion element and the evaporator.

2.2 Mathematical calculations and equations:

Evaporator capacity

$$Q_L = \dot{m}_R(h_1 - h_4) \quad (1)$$

$$\mathrm{Q_L} = \mathrm{Q_H} - \mathrm{W_{Comp}} \quad (2)$$

Fluid flow rate

$$\dot{m}_R = \frac{Q_L}{(h_1 - h_4)} \quad (3)$$

Condenser capacity

$$Q_H = \dot{m}_R(h_2 - h_3) \quad (4)$$

$$Q_H = Q_L + W_{Comp} \quad (5)$$

The heating or cooling performance coefficient (COP) is determined by dividing the heating or cooling load generated by the energy consumed.

$$\mathrm{COP} = \frac{\mathrm{Q_L}}{\mathrm{W_{Comp}}} = \frac{\mathrm{h_1 - h_4}}{\mathrm{h_2 - h_1}} \quad (6)$$

2.3 Real Vapor Pressure Refrigeration Cycle:

There are some differences between an actual vapor pressure refrigeration cycle and an ideal cycle. This difference is mostly due to the irreversibility (the absence of heat and pressure loss) of the components that make up the cycle. Two main sources of irreversibility are the coefficient of friction between the refrigerant and the inner pipe surface, and the undesirable heat exchange with the external environment, excluding the evaporator and condenser.

In an ideal cycle, the vapor exiting the evaporator enters the compressor as saturated vapor. However, this condition (saturated vapor) cannot be fully guaranteed in an actual cycle, as it is nearly impossible to precisely control the state of the vapor phase. Instead, the system must be designed so that there is some superheated vapor at the compressor inlet of the refrigerant gas. The purpose here is to prevent the liquid from transferring to the compressor. Also, the connection between the evaporator and compressor is usually maintained for heat exchange, where the cold gas coming from the evaporator and entering the compressor is heated via a heat exchanger through which the hot gas exiting the compressor passes (superheating), and the hot gas coming from the condenser and entering the evaporator is cooled via a heat exchanger through which the cold gas exiting the evaporator passes (subcooling). In this way, the pressure loss due to friction and heat transfer from the environment to the liquid becomes significant, and these effects will also increase the specific volume of the liquid and the working power required from the compressor [23].

The two most important factors in using cascade refrigeration systems are cost and energy efficiency. Cooling at extremely low temperatures using a single-stage cycle requires larger compressors and more expensive materials. In addition to the high cost, cooling efficiency at very low temperatures with a single-compressor system will be lower, and energy consumption will be higher. In contrast, with cascade refrigeration systems, cooling at low temperatures can be achieved by running two refrigeration cycles at a lower cost.

As clearly shown in the T-S and P-h diagrams in Figures (2&3), the compressor workload decreases with sequential operation, while the heat drawn from the refrigerated environment increases. Therefore, sequential operation increases the efficiency coefficient of the refrigeration system.

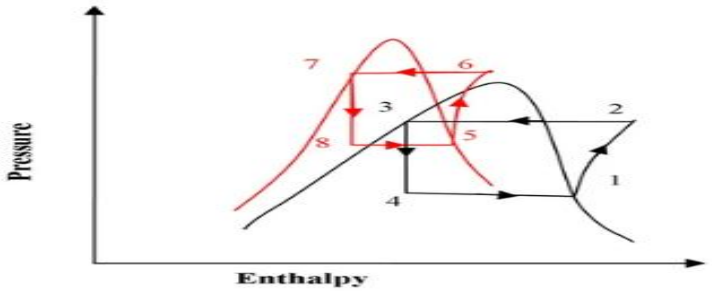

Figure (2) P-h diagram of cascade refrigeration system

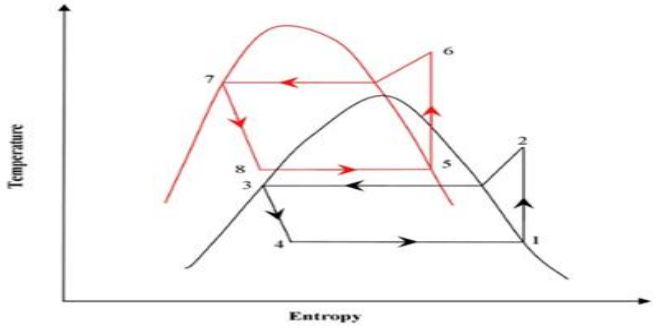

Figure (3) T-s diagram of a cascade refrigeration system

Flow rate ratio of refrigerants for a sequential cooling system:

$$\dot{m}_{HPC}(h_6 - h_7) = \dot{m}_{LPC}(h_2 - h_3) \quad (7)$$

$$\frac{\dot{m}_{HPC}}{\dot{m}_{LPC}} = \frac{h_2 - h_3}{h_6 - h_7} \quad (8)$$

Efficiency coefficient of the cascade system:

$$COP = \frac{Q_L}{W_{net}} = \frac{\dot{m}_{LPC}(h_1 - h_4)}{\dot{m}_{HPC}(h_6 - h_5) + \dot{m}_{LPC}(h_2 - h_1)} \quad (9)$$

$$COP = \frac{Q_L}{W_{Comp.HPC} + W_{Comp.LPC}} \quad (10)$$

Superheat

As illustrated in Figure 4, when the refrigerant in the cycle is in the gaseous state at a temperature higher than the temperature corresponding to the vapor pressure, this is called "superheating." For example, if we take water molecules (H_2O), they boil at 100°C under normal atmospheric conditions to vaporize. However, if they can absorb more heat before vaporizing, the vapor temperature will exceed 100°C. This vapor is called superheated steam, and this process is called "superheating."

Libyan Open University Journal of Applied Sciences (LOUJAS)
Volume 2 - Issue 1 - 2026 - Pages 274-289

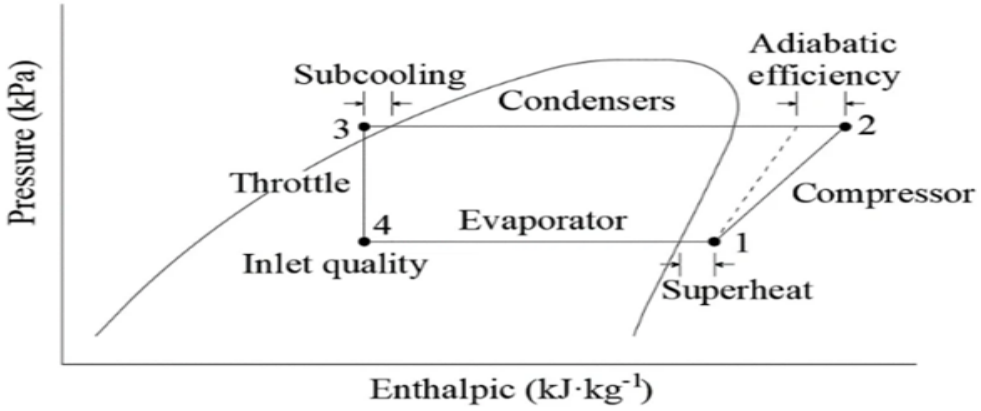

Figure 4 Application of superheating to the P-h diagram

Superheating is represented on the pressure-enthalpy (P−h) diagram as a horizontal straight line (constant pressure) extending to the right of the saturation curve (the superheated vapor region). This movement represents an increase in the enthalpy (h) of the vapor at a constant vapor pressure, ensuring complete evaporation of the refrigerant and protecting the compressor from fluid. The lines in the superheating region to the right of the inverted U-shaped saturation curve show a deviation from the constant pressure and constant temperature lines, indicating an increase in temperature and enthalpy. Technicians use these lines to adjust the performance of thermal expansion valves. When comparing high versus low superheating, high superheating indicates a low coolant volume or an overload, leading to premature evaporation, while low superheating may indicate an overload or overfeed, potentially resulting in coolant backflow. The thermodynamic definition of superheating is that steam is considered superheated if it is heated to a temperature above its boiling point. As shown in Figure 3, the sensible coolant temperature rises as a result of superheating. System efficiency is crucial in determining compressor lifespan and maximum capacity. High superheat values are not always desirable. Although ideal superheat values vary depending on the cycle used, they generally range between 3°C and 15°C.

The superheat is controlled by the flow rate of the fluid through the evaporator, and the expansion element is crucial here. Thermal expansion valves (TEV), automatic expansion valves (AEV), or electronic expansion valves (EEV) are used to control the fluid flow through the evaporator. However, effective control of superheating is not possible with expansion elements such as capillary tubes, where no adjustments can be made [22]. This delicate balance ensures that the superheat is maintained at a constant level, protecting the compressor and improving cooling efficiency.

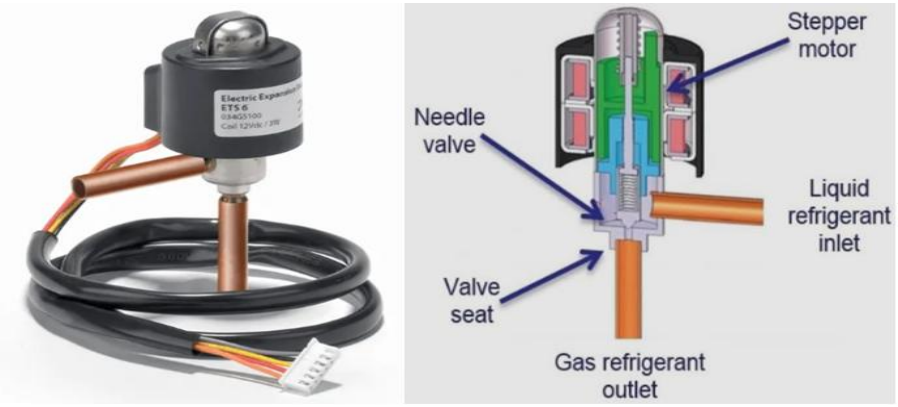

Figure 5 shows a cross-section of an electronic expansion valve

The electronic expansion valve (EEV) is a precision device in refrigeration and air conditioning systems that effectively controls the flow of refrigerant (Freon) to the evaporator using a stepper motor and an electronic control unit in response to temperature and pressure. It ensures high efficiency, stable superheating, and prevents refrigerant backflow to the compressor.

3 Materials and Methods:

This section describes the cycle elements that make up the experimental setup and their characteristics. Using the auxiliary cycle elements and electronic expansion valves described earlier aims to make the experimental setup more controlled. Electronic expansion valves were used in both cycles, and their features were explained previously. The evaporator in the high-temperature cycle functions as a series plate heat exchanger. The condenser in LPC also functions as a series plate heat exchanger. Although it is not possible to accurately calculate the capacity of the heat exchanger used in CRS, the most suitable capacity can be determined experimentally, this is because the enthalpy of the coolant is not constant in both systems.
The volume of fluid passing through the heat exchanger will be relatively lower compared to single-flow refrigeration systems, a high-turbulence, cross-pass (H-type) heat exchanger is chosen. This design aims to allow the refrigerant to transfer more heat within the exchanger. H-type plates can increase pressure loss due to the high turbulence they generate, thus maximizing heat transfer with turbulence in low-flow systems. The pressure loss is lower in low-flow systems than in high-flow systems, turbulence is preferred in the heat exchanger.

3.1 Theoretical calculations of the experimental system:

Prior to designing the experimental setup, theoretical analyses of the experimental setup were conducted. The "Coolpack" software, developed in collaboration with the IPU and the Department of Mechanical Engineering Technical University of Denmark, is an Excel-based analysis program. For the analyses, version 1.49 of "Coolpack" was used, which includes a feature for analyzing the cascade cooling cycle. The input parameters used in the program are listed in Table 1 below.

Table 1: The input of values into the Coolpack program:

Parameters	Values
$\boldsymbol{Q_{LPC,Evap}}$	1000 W
$\boldsymbol{W_{LPC,Comp}}$	4260 W
LPC R32 evaporation temperature	-50 °C
LPC R32 condensation temperature	15 °C
LPC compressor isentropic efficiency	0,8
LPC Superheat temperature	4 °C
LPC Subcooling temperature	2 °C
HPC R407c evaporation temperature	5 °C
HPC R407c condensing temperature	45 °C
HPC compressor isentropic efficiency	0,8
HPC Superheat temperature	4 °C
HPC Subcooling temperature	2 °C

The equations used by the Coolpack software in the thermodynamic analysis of the system are listed below:

Compressor capacities:

$$W_{LPC} = \dot{m}_{LPC} \times (h_2 - h_1) \quad (11)$$

$$W_{HPC} = \dot{m}_{HPC} \times (h_6 - h_5) \quad (12)$$

$$h_3 = h_4 \quad (13)$$

Calculating capacitor capacity:

$$Q_{Cond,LPC} = \dot{m}_{LPC} \times (h_2 - h_3) \quad (14)$$

$$Q_{Cond,HPC} = \dot{m}_{HPC} \times (h_6 - h_7) \quad (15)$$

Evaporator capacity calculation:

$$Q_{\text{Evap},LPC} = \dot{m}_{LPC} \times (h_1 - h_4) \quad (16)$$

$$Q_{\text{Evap},HPC} = \dot{m}_{HPC} \times (h_5 - h_8) \quad (17)$$

Performance rate:

$$COP_{LPC} = \frac{Q_{evap,LPC}}{W_{comp,LPC}} \quad (18)$$

$$COP_{HPC} = \frac{Q_{evap,HPC}}{W_{comp,HPC}} \quad (19)$$

Plate heat exchanger calculation:

$$\dot{m}_3 = \dot{m}_4 \quad (20)$$

$$\dot{m}_7 = \dot{m}_8 \quad (21)$$

$$\dot{m}_2 \times (h_2 - h_3) = \dot{m}_6 \times (h_6 - h_7) \quad (22)$$

$$\dot{m}_L \times Q_L = \dot{m}_H \times Q_H \quad (23)$$

4. Implementing Experiment:

Leakage tests were performed before filling the laboratory system with gas at the weld joints. In the leakage test, the pressure in both cycles was initially raised to 15 bar and then maintained at that pressure for one day. Pressure gauges on the assembly and service pressure values were checked, and a foam test was performed on all weld points. After the pressure tests, the pressure in both cycles was reduced to -1 bar using a vacuum pump, and the system was vacuum-cleaned for 30 minutes at this pressure.

After the cycles, which had been performed at a vacuum pressure of at least -1 bar for one day, successfully passed these tests, the optimal gas charge was achieved by gradually charging the refrigerant.

Before welding the copper piping system, the circuit components were installed. All welding operations in the laboratory system were then completed using oxyacetylene and silver-copper welding.

4.1 Measuring and recording experimental data:

Temperature values were measured and recorded at various points within the experimental setup using a data logger. Thermocouples were connected to the Ordel UDL200 at ten different points within the experimental setup. An Ordel SBA200 RS485-USB adapter was used to transfer the measurements to a computer. Temperature values were recorded using Ordel's Dali 485 computer interface software. The software interface allows for saving and exporting measured values to Excel. In order to conduct experimental measurements in the

designed and manufactured experimental setup, two computer-controlled cold chamber controllers, thermocouple temperature sensors, and an electronic electricity meter are used.
Experimental measurements were not taken in cases where ambient weather conditions differed. In each experiment, the superheating setting values for both cycles were kept equal at 4°C. Each experiment was conducted in eight-hour periods at the same time of day.
The constant factor in the experimental sequence was convection in the refrigerator. In each experiment, 15 plastic water bottles with a capacity of 500 cc were used as convection. The position of the bottles in the reservoir was kept constant, and the water temperature was continuously measured and recorded by placing a thermocouple temperature sensor inside the water bottle.
Before each experiment, it was confirmed that the cold room and water bottles were in thermal equilibrium with the laboratory's climatic conditions. At least one day was allowed between experiments to allow for the equilibrium of temperature and pressure values. The experiments were conducted at the same time of day, and only one experiment was performed on any given day. The accuracy of the measuring instruments used in the experimental setup was verified before the experiments, and the same measuring instruments were used in all experiments. Power was supplied to the cycle elements in the experimental setup from a single point, and energy consumption was measured using a digital electricity meter. The measuring instruments and computer were supplied by different manufacturers. All experiments were conducted over a duration of 8 hours.
The records taken from the computer-connected measuring devices were transferred to Excel format. Records were taken at 60-second intervals, and the arithmetic mean was calculated for each 5-minute recording. Experimental and recording charts were created with 5-minute values, and curves were plotted for each hour. Energy consumption values were read manually from the electronic meter and recorded every 10 minutes.

Table 2 :shows the installation points of the temperature and pressure sensors recorded during the experiments, totaling 15 points:

HPC Compressor outlet temperature	LPC heat exchanger inlet temperature
HPC Condenser Inlet Temperature	LPC heat exchanger outlet temperature
HPC Condenser outlet temperature	EGV (Electronic expansion valve)
EGV (Electronic expansion valve)	LPC Evaporator outlet temperature
HPC heat exchanger inlet temperature	Refrigerator room temperature
HPC heat exchanger outlet temperature	LPC Evaporator outlet temperature
HPC Evaporation pressure sensor	LPC Evaporation pressure sensor
LPC Compressor outlet temperature	

The phase state and temperature of the steam entering the compressor are critical factors in compressor energy consumption. In steam compressors, the incoming steam must be in a superheated steam phase. When the refrigerant enters the compressor in a liquid state, the compressor oil temperature drops and its viscosity is affected. This change in viscosity leads to increased energy consumption due to friction, and the compressor will eventually fail.

5. Results and discussion

Figure 6 illustrates the temperature decrease in the refrigerant chamber after two hours of operation, up to eight continuous hours of thermostat-free operation. Figure 6 shows that R32 reaches -26°C after two hours of operation, while the mixture reaches -28°C at the same time.

This indicates that the mixture is more suitable for use in refrigerators with a temperature of -29°C, as it reaches this temperature more quickly than R32. After six hours of operation, in both experiments, the refrigerant reaches -29.25°C, demonstrating that the mixture reaches this temperature faster and is less harmful to the environment than R32. During the last two hours, the performance of both refrigerants is similar, with the temperature in the refrigerated chamber decreasing from -29.25°C to -31.75°C by the end of the eighth hour.

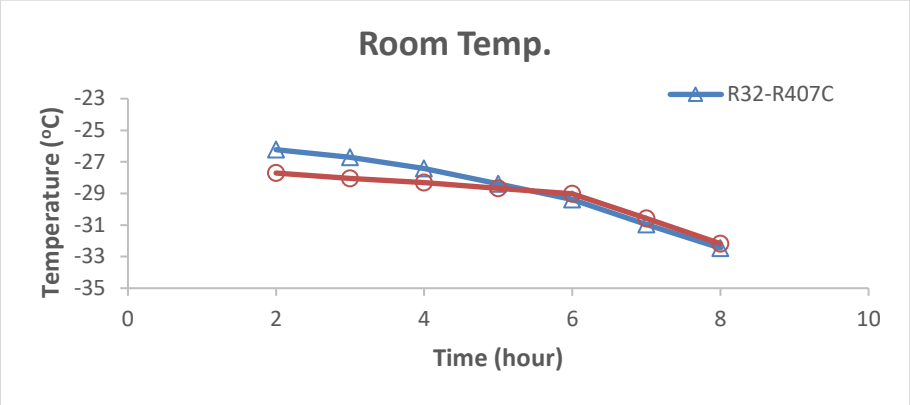

Figure 6 Refrigerated Room Temperature

Figure 7 shows the pressure drop along the suction line in the low-pressure cycle, reaching its highest value for R32 at 1.83 bar. From there, it drops smoothly and gently to 1.6 bar by the end of the fifth hour. R32 during the two hours from the end of the fifth hour to the end of the seventh hour, the drop is steeper, reaching 1.4 bar. For the final hour of the curve, the drop is steepest, reaching 1.2 bar at the end of the first experiment.

In the second experiment, Figure 7 shows that when using the mixture, the suction line pressure is 1.7 bar, which is 0.13 bar lower than the pressure for R32 at the end of the second hour of operation. Over the course of the second hour, it rises by only 0.05 bar, a value lower than the pressure for R32 at the end of the second hour. From the end of the third hour to the end of the fifth hour, the pressure gradually decreases to 1.68 bar, where it remains constant for the next hour. From the end of the sixth hour to the end of the seventh hour, there is a sharp drop, reaching its lowest value when using the mixture, which is 1.4 bar. During the last hour of the curve, the pressure rises slightly by 0.02. As can be seen from Figure 10, there is a direct relationship between evaporation pressures and superheat values.

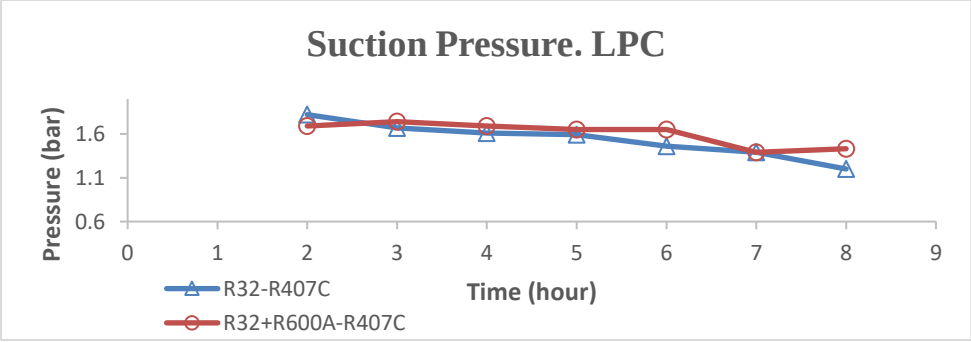

Figure 7 Suction line pressure in LPC

Figure 8 shows the pressure drop along the suction line in HPC. The blue curve illustrates the smooth pressure drop of R407c in the suction line during the first experiment with R32. The blue curve decreases from 3.07 bar to 2.83 bar during the six-hour operating period recorded in the first experiment. Although LPC fluid pressures are affected later than HPC fluid pressures, the effect of roasting values on evaporation pressure is different.

In the second experiment, using HPC, the suction line pressure, shown in red, exhibits a slight increase during the first three hours of the curve, from 3.05 bar to 3.1 bar. The highest pressure on the curve is observed for R407c gas when the mixture is used, reaching 3.18 bar

at the end of the sixth hour. During the final two hours of the curve, the suction line pressure in LPC decreases from 3.18 bar to 2.98 bar at the end of the curve.

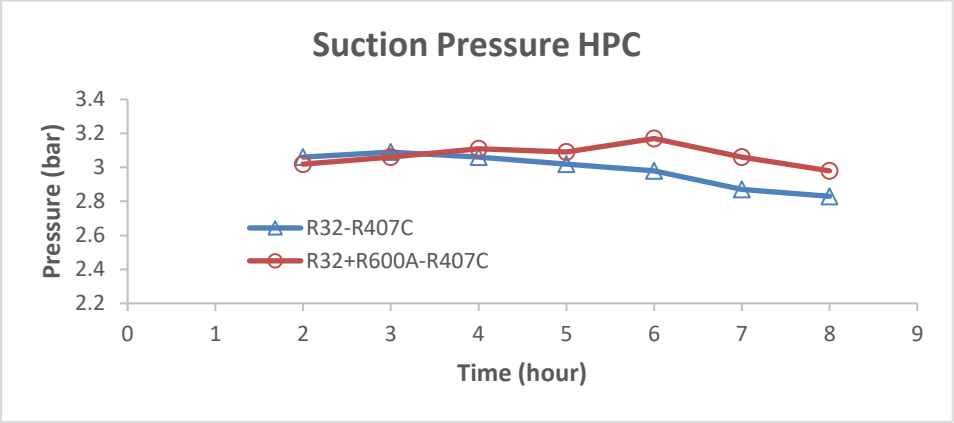

Figure 8 Suction line pressure in HPC

Figure 9 shows the percentage of valve opening over time during LPC. The curve in the first experiment using R32 is more consistent than the curve in the second experiment using the mixture, this difference is due to the difference in composition between R32 and the mixture components. The curve representing the valve opening percentage for R32 starts at 8.5%, then decreases to 7% during the first hour. In the second hour, the valve opening percentage increases slightly by 0.5%. The valve opening percentage then declines more rapidly during the following two hours, following the same gradual progression from 7.5% to 5.4%. During the final two hours, the valve opening percentage reaches 6.2% with a steady increase.

For the mixture, the purple curve in Figure 9 shows an irregular graph of the valve opening percentage in the second experiment due to the composition of the mixture's components. The curve starts at a valve opening of 9.2%, then drops to 6.2% in the first hour, which is the lowest valve opening percentage in the second experiment when using the mixture. During the three hours, from the end of the third hour to the end of the sixth hour, the valve opening percentage increases at a nearly regular rate to reach 11%. Thru the last two hours, there is a wave-like decrease and increase from 11% to 8.2% during the seventh hour, then it returns to 11% during the final hour. In the HPC refrigerant, unlike the LPC refrigerant, there is an inverse relationship between the superheating value and the evaporation pressure, this is due to differences in the thermodynamic properties of the fluids and the lower fluid flow rates.

Although there are fluctuations in the pressure curves, it is generally observed that the pressure decreases proportionally with room temperature. These fluctuations in the pressure curves are due to the rate of heat transfer in the heat exchanger and small changes in room temperature.

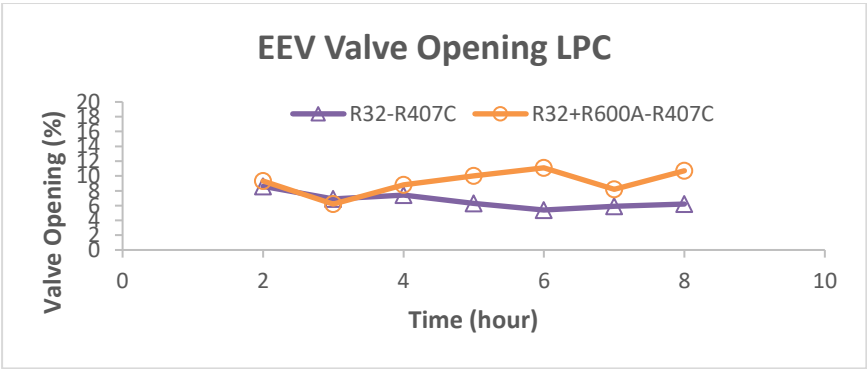

Figure 9 shows the opening of the expansion valve in LPC

Figure 10 illustrates superheat in the suction line, determined and controlled by the computer at 4°C. Both curves show the rise and fall of superheat value as a result of the potential evaporation of liquid refrigerant present in the suction line, controlled by the expansion valve opening ratio. The added heat values shown in the diagram are the result of precise computer control of the expansion valve opening ratio. The valve opens whenever superheat value falls below 4°C and closes when superheat exceeds 4°C, as determined by sensors installed in the suction line at the compressor inlet.

Figure 10 shows a similarity in both experiments during the hour from the end of the second hour to the end of the third hour, decreasing from 5°C to 3.1°C. During the fourth hour, a difference appears between the two curves due to the different compositions of the two fluids. The blue curve, representing R32, rises, and the red curve, representing the mixture, falls during the fourth hour.

Superheat value at the end of the fourth hour using R32 is 4.4°C. During the fifth hour, superheat value remains stable at 4°C. In the course of the last three hours, there is a slight increase in superheat of 0.5°C by the end of the seventh hour, before it drops to 4°C in the final hour.

The lowest temperature added in the second experiment using the mixture is 3 degrees Celsius, reaching this level at the end of the fourth hour. The red curve begins to rise from the end of the fourth hour, continuing for two full hours to reach 5.8 degrees Celsius at the end of the sixth hour of operation. The curve representing the second experiment then drops to 3 degrees Celsius during the seventh hour, after which it rises again to 5.7 degrees Celsius by the end of the experiment.

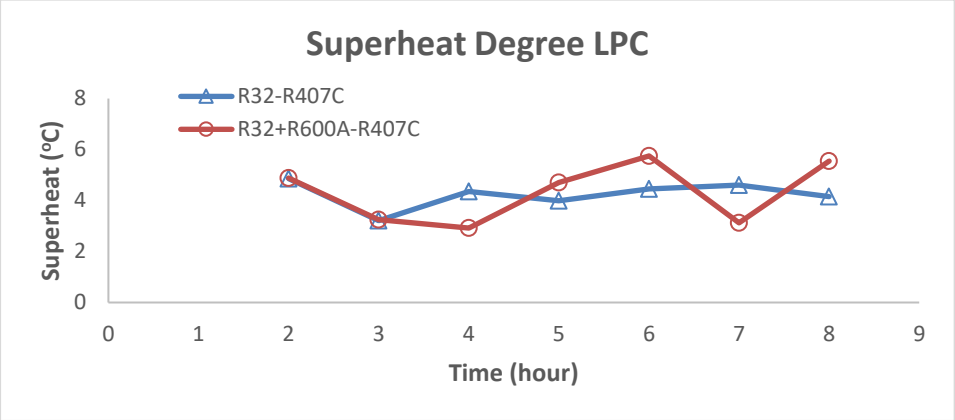

Figure 10 Heat added by low-pressure cycle

Figure 11 shows a double comparison with the first experiment using R32, the computer-controlled additive temperature of 4°C, and the percentage of valve opening. The electric expansion valve opens when the suction line temperature rises above 4°C until it drops to 4°C. Similarly, the valve closes when the additive temperature falls below 4°C until the suction line is balanced. Figure 11 demonstrates the correlation and consistency between the two curves, indicating precise control of the additive temperature, which allows us to maintain the entry of the refrigerant gas into the compressor without it containing liquid. At 4.9°C, the highest superheat in the first experiment, the valve opening percentage is 8.5%. Throughout the third hour, the curve showing superheat drops sharply to 3.2°C, followed by a decrease in the valve opening percentage to 7%. At the end of the fourth hour, there is a continuous increase in superheat from 3.2°C to 4.3°C, approximately 1°C, and a slight increase in the valve opening percentage from 7% to 7.3%. Through the fifth hour, both curves decrease slightly. The relationship between superheat and the valve opening percentage is that the higher superheat, the greater the valve opening; that is, the relationship is directly proportional, as clearly demonstrated during the last three hours.

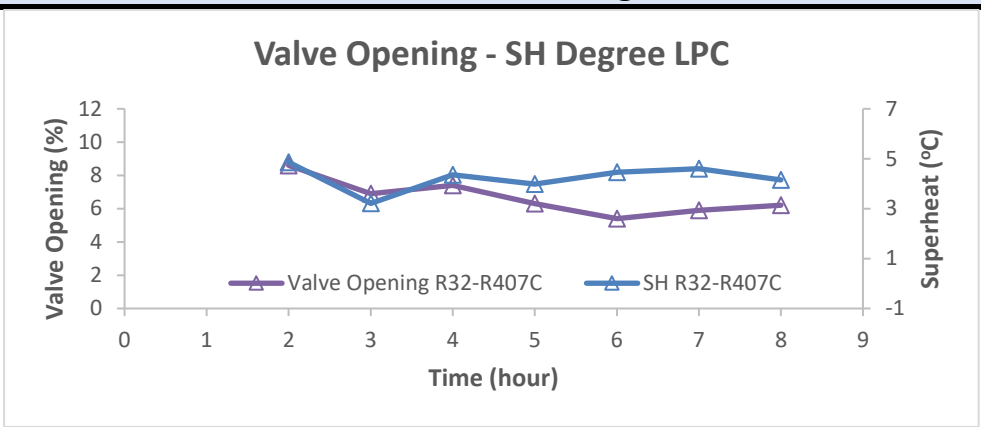

Figure 11 the valve opening with superheat in LPC of R32

Figure 12 shows a valve opening value of 9.4% at the beginning of the valve opening ratio curve which shown in orange at superheat of 4.9°C. In the third hour, it decreases to 6.2% at a heating temperature of 3.2°C. At the fourth hour, superheat decreases slightly by 0.3°C, while the valve opening ratio increases to 8.8%. This fourth hour indicates that the evaporator requires more refrigerant fluid, which contains different proportions of the two gases in the mixture, passing through the electronic expansion valve, while superheat is very close to the computer-defined value of 4°C. At the fifth and sixth hours, the relationship between the two curves increases from 8.8% to 11.4%, the highest value for valve opening in the experiment. Similarly, the heat additive increases from 2.8°C to 5.8°C, the highest superheat recorded in the second experiment.

The added temperature value increases when the compressor outlet temperature rises, at which point it comes into contact with the suction line as a heat exchanger. It decreases as the compressor outlet temperature decreases. In the course of the last two hours, there is a sharp drop at hour seven and a sharp rise at hour eight. The sharp drop is explained by the evaporator reaching its full refrigerant content, at which point the electrical expansion valve closes when superheat reaches 4°C. The highest superheat is 5.6°C at the end of the red curve after eight hours of operation.

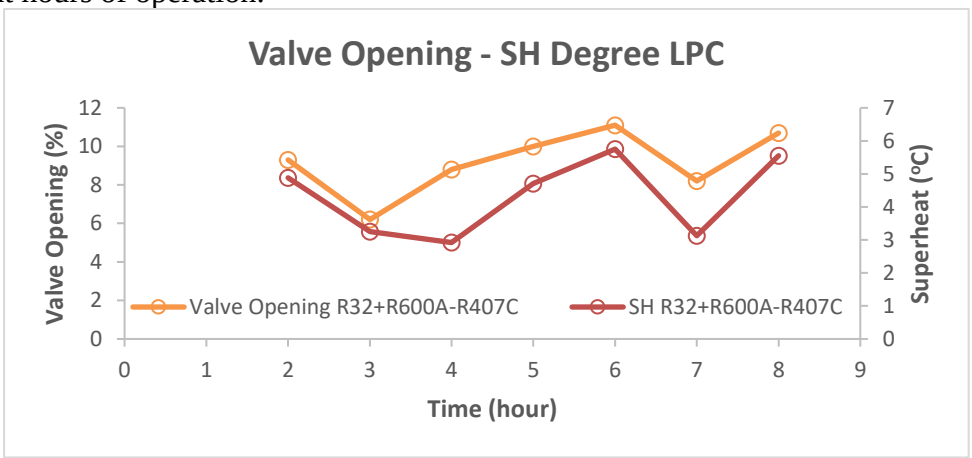

Figure 12 Valve opening with superheat in LPC of the mixture

Conclusion

As the superheating values increase, the fluid flow rates decrease. Consequently, a reduction in heat transfer in the heat exchanger was observed. Furthermore, tests revealed that the evaporation pressure of R407C fluid is external climatic conditions. Therefore, particular attention was paid to conducting experiments under the most environmentally friendly

conditions. Condenser temperature measurements were taken in LPC from the evaporator outlet of the heat exchanger and in HPC from the condenser outlet of the heat exchanger. Several factors influence LPC heat exchanger outlet temperatures, including the heat transfer rate, the instantaneous thermodynamic properties of the fluids, and evaporation temperatures. However, it is clear that the heat exchanger outlet temperatures are not directly related to the cold room temperature but rather to the amount of heat transferred achieved in the heat exchanger.

With a decrease in the EEV valve openings, the amount of heat transferred decreases and the fluid flow rate. Therefore, in LPC fluid, as the superheating temperature increases, the condenser outlet temperature rises due to the decreased fluid flow rate and the inability to dissipate heat. In HPC the flow rate decreases as the superheating temperature increases. It has been determined that condenser outlet temperatures decrease as the heat transfer rate in the heat exchanger decreases. It has also been established that condenser outlet temperatures are related to the amount of heat transferred by the heat exchanger as well as the evaporator pressure.

Recommendations:

While the highest power consumption was 1943 kW with the LPC experiment, the lowest power consumption was 1675 kW with the HPC experiment, representing a 13.8% decrease in consumption. These results indicate that superheat values play a significant role in power consumption.

Due to the added temperature variations and the high probability of fluid flow into the compressor, it was observed that a collector (liquid trap) should be used in both cycles in successive cycles.

While there is a direct relationship between the LPC evaporation pressure and the cold room temperature, it was determined subsequently affected by the HPC pressure. Furthermore, it was observed that the LPC and HPC evaporation pressures give different responses to superheat values, and the optimal superheat values will also differ. It was observed that the temperature of the cold room is not directly related to the condenser outlet temperature, but rather to the amount of heat dissipated in the condenser.

While HPC fluid is more affected by ambient temperature, LPC fluid is primarily affected by the heat transfer rate in the heat exchanger. Considering energy consumption, ambient temperature, compressor outlet temperature, and COP values, a superheating value of 4°C was observed, with experimental results revealing more optimal data.

Suggestions:

According to the results, the added heat in successive cooling cycles significantly impacts efficiency and energy consumption. Determining the optimal temperatures for each cycle separately using an automated system can enhance system efficiency. By comparing this study with different refrigerants, it can be determined whether there is a difference in the optimal refrigerant temperatures. Various improvements can be made to the heat exchanger to reduce the LPC cycle equilibrium time in successive cycles and achieve the desired room temperatures in less time.

References

[1] KESHTKAR, Mohammad Mehdi. Effect of subcooling and superheating on performance of a cascade refrigeration system with considering thermo-economic analysis and multi-objective optimization. Journal of Advanced Computer Science & Technology, 2016, 5.2: 42-47.

[2] HÝL, Radim; WAGNEROVÁ, Renata. Design and implementation of cascade control structure for superheated steam temperature control. In: 2016 17th International Carpathian Control Conference (ICCC). IEEE, 2016. p. 253-258.

[3] JARHULT, Casper. Modeling and Control System Design of a Cascade Vapor Compression System. 2025.

[4] MUSSATI, Sergio F.; MOROSUK, Tatiana; MUSSATI, Miguel C. Superstructure-based optimization of vapor compression-absorption cascade refrigeration systems. Entropy, 2020, 22.4: 428.
[5] BOAHEN, Samuel; CHOI, JongMin. Research trend of cascade heat pumps. Science China Technological Sciences, 2017, 60.11: 1597-1615.
[6] CALISKAN, Hakan; HONG, Hiki; JANG, Jin Kyung. Thermodynamic assessments of the novel cascade air cooling system including solar heating and desiccant cooling units. Energy Conversion and Management, 2019, 199: 112013.
[7] QUEIROZ, Marcus Vinicius Almeida, et al. Experimental comparison of a cascade refrigeration system operating with R744/R134a and R744/R404a. 2016.
[8] FAN, Chenghao; PEI, Dongsheng; WEI, Hongqi. A novel cascade energy utilization to improve efficiency of double reheat cycle. Energy Conversion and Management, 2018, 171: 1388-1396.
[9] KUMAR, Sachin; RANGA, Vicky. Work study on low temperature (cascade) refrigeration system. Int. Res. J. Eng. Tech, 2018, 5: 2300-2305.
[10] SOBIERAJ, Michał; ROSIŃSKI, Marian. High phase-separation efficiency auto-cascade system working with a blend of carbon dioxide for low-temperature isothermal refrigeration. Applied Thermal Engineering, 2019, 161: 114149.
[11] HU, Kaiyong, et al. Effects of evaporator superheat on system operation stability of an organic Rankine cycle. Applied Thermal Engineering, 2017, 111: 793-801.
[12] ZHU, Jie; HUANG, Hulin. Performance analysis of a cascaded solar Organic Rankine Cycle with superheating. International Journal of Low-Carbon Technologies, 2016, 11.2: 169-176.
[13] YIN, Xiaohong, et al. Energy-efficiency-oriented cascade control for vapor compression refrigeration cycle systems. Energy, 2016, 116: 1006-1019.
[14] MIAO, Qing, et al. Wide operating temperature range vapor compression/auto-cascade heat pump air conditioning system adopting zeotropic mixtures: Feasibility analysis. Energy and Buildings, 2025, 116732.
[15] YILMAZ, Barış; MANÇUHAN, Ebru; YILMAZ, Deniz. Theoretical analysis of a cascade refrigeration system with natural and synthetic working fluid pairs for ultra low temperature applications. Isı Bilimi Ve Tekniği Dergisi, 2020, 40.1: 141-153.
[16] WANG, Wenyi, et al. The intermediate temperature optimization for cascade refrigeration system and air source heat pump via extreme seeking control. International Journal of Refrigeration, 2020, 117: 150-162.
[17] XU, Yingjie, et al. Thermodynamic analyses and performance improvement on a novel cascade-coupling-heating heat pump system for high efficiency hot water production. Energy Conversion and Management, 2023, 293: 117448.
[18] LIU, Changxin, et al. Influence study of bottom cycle ratios and superheat for vessels waste heat cascade recovery based on TEG-ORC combined cycle system employing R245fa. International Journal of Green Energy, 2023, 20.7: 734-743.
[19] LI, Ruishen, et al. Theoretical analysis of three CO2/C3H8 (R744-R290) cascade refrigeration systems with precooling processes in low-temperature circuits. Applied Thermal Engineering, 2023, 234: 121238.
[20] KEZIER, Deliya, et al. A semi-cascade heat pump system for different temperature lifts. Applied Thermal Engineering, 2024, 236: 121767.
[21] YERDESH, Ye, et al. Numerical simulation on solar collector and cascade heat pump combi water heating systems in Kazakhstan climates. Renewable Energy, 2020, 145: 1222-1234.
[22] YINLONG, Li, et al. Experimental study on the performance of an auto-cascade refrigeration system integrating fractional condensation and flash separation. Energy, 2025, 332: 137021.
[23] DA SILVA, Alessandro; BANDARRA FILHO, Enio Pedone; ANTUNES, Arthur Heleno Pontes. Comparison of a R744 cascade refrigeration system with R404A and R22 conventional systems for supermarkets. Applied Thermal Engineering, 2012, 41: 30-35.